Synthesis of Mixed Copper−Zinc Basic Carbonates and Zn-Doped Tenorite by Homogeneous Alkalinization

Galo J. de A. A. Soler-Illia,[†] Roberto J. Candal,[†] Alberto E. Regazzoni,*[,‡] and Miguel A. Blesa[†,‡]

INQUIMAE, Facultad de Ciencias Exactas y Naturales, Universidad de Buenos Aires, Pabellón II, Ciudad Universitaria, 1428-Buenos Aires, Argentina, and Unidad de Actividad Química, Comisión Nacional de Energía Atómica, Av. del Libertador 8250, 1429-Buenos Aires, Argentina

Received May 15, 1996. Revised Manuscript Received October 1, 1996[⊗]

Spherical equally sized mixed copper−zinc basic carbonates and Zn-doped tenorite particles have been prepared by coprecipitation from copper−zinc nitrate solutions that become homogeneously alkaline by the hydrolysis of urea at 363 K. The nature of the synthesized solids depends on the initial zinc to total metal mole ratio (X_{Zn}) and aging time. At short aging times, amorphous copper hydroxide particles, with variable carbonate and zinc contents, precipitate irrespective of initial solution composition. The subsequent evolution of this amorphous precursor is strongly affected by X_{Zn}. At low zinc contents, i.e., $X_{Zn} = 0.06$, a mixture of zincian−malachite and Zn-doped tenorite forms; both solids have the same zinc content, which is 4.0 mol %. Upon further aging, zincian−malachite dissolves and Zn-doped tenorite grows. In the range $0.50 \geq X_{Zn} > 0.30$, on the other hand, only aurichalcite forms; the final solid composition is essentially that of the starting solution. Mixtures of aurichalcite, zincian−malachites and Zn-doped tenorite, in varying proportions, form at intermediate X_{Zn} values. The evolution of the studied systems is contrasted against the precipitation behavior of the individual metal ions. Such a comparison shows that copper and zinc nucleation are separate events, which are little influenced by each other. The thermodynamic and kinetic factors that determine the overall evolution of the systems are thoroughly discussed.

Introduction

Currently, much attention is paid to "traditional" materials, i.e., materials that have been used for a long time, in an effort to prepared microcrystalline solids composed of particles well defined in composition, size and shape. The extensive work by Matijević has cleared the pathway to synthesize uniform metal oxide particles, and has shown how the properties of the materials can be substantially improved by controlling particle size and shape.[1−3] The homogeneous alkalinization of salt solutions by the hydrolysis of urea is a very suitable method to synthesize a wide variety of metal oxides, either directly, or via the formation of a solid precursor. The method allows for the easy control of the rate of supersaturation increase and permits the synthesis of well-defined equally sized particles once the appropriate conditions to produce just one burst of nuclei formation have been set.[4−12] The possibilities and limitations of the *urea method* to prepare precursors of mixed metal oxide powders have been addressed in previous works.[13−15] The main limitations, certainly shared by other coprecipitation procedures, are posed by the hydrolytic properties of the metal ions to be coprecipitated.[16,17] Indeed, their hydrolytic behaviors reflect themselves in nucleation and growth kinetics. Thus, simultaneous nucleation is seldom the case, and usually a phase containing only one cation nucleates first to later serve as the locus for the heterogeneous nucleation of a second solid, which grows incorporating both cations at different rates. As a result, the composition of the synthesized precursors is not homogeneous. This limitation may be easily circumvented by subsequent thermal treatment, provided there is no phase segregation. However, in most usual cases, various solid phases (of different compositions) may form through parallel pathways, and the setting of the most suitable synthesis conditions requires of a detailed experimental exploration.

[†] Universidad de Buenos Aires.
[‡] Comisión Nacional de Energía Atómica.
[⊗] Abstract published in *Advance ACS Abstracts,* December 1, 1996.

(1) Matijević, E. In *Science of Ceramic Chemical Processing*; Hench, L. L., Ulrich, D. R., Eds.; Wiley: New York, 1986; p 463.
(2) Matijević, E. In *Ultrastructure Processing of Advanced Ceramics*; MacKenzie, S. D., Ulrich, D. R., Eds.; Wiley: New York, 1988; p 429.
(3) Matijević, E. *Langmuir* **1994**, *10*, 8.
(4) Cornilsen, B.; Reed, J. *Am. Ceram. Soc. Bull.* **1979**, *58*, 1199.
(5) Blendel, J.; Bowen, H. K.; Coble, R. *Am. Ceram. Soc. Bull.* **1984**, *63*, 797.
(6) Janeković, A.; Matijević, E. *J. Colloid Interface Sci.* **1985**, *103*, 436.
(7) Akinc, M.; Sordelet, D. *Adv. Ceram. Mater.* **1987**, *2*, 232.
(8) Matijević, E.; Hsu, W. P. *J. Colloid Interface Sci.* **1987**, *118*, 506.
(9) Sordelet, D.; Akinc, M. *J. Colloid Interface Sci.* **1988**, *122*, 47.
(10) Castellano, M.; Matijević, E. *Chem. Mater.* **1989**, *1*, 78.
(11) Kratohvil, S.; Matijević, E. *J. Mater. Res.* **1991**, *6*, 766.
(12) Candal, R. J.; Regazzoni, A. E.; Blesa, M. A. *J. Mater. Chem.* **1992**, *2*, 657.
(13) Aiken, B.; Hsu, W. P.; Matijević, E. *J. Am. Ceram. Soc.* **1988**, *71*, 845.
(14) Ribot, F.; Kratohvil, S.; Matijević, E. *J. Mater. Res.* **1989**, *4*, 1123.
(15) Candal, R. J.; Regazzoni, A. E.; Blesa, M. A. *Colloids Surf. A* **1993**, *79*, 191.
(16) Blesa, M. A.; Soler-Illia, G. J. de A. A.; Candal, R. J.; Regazzoni, A. E. In *Fine Particles Science and Technology*; Pelizzetti, E., Ed.; Kluwer: Dordrecht, 1996; p 33.
(17) Candal, R. J. Ph.D. Thesis, Universidad de Buenos Aires, Argentina, 1995.

S0897-4756(96)00281-5 CCC: $14.00

Classical coprecipitation procedures have been used to prepare precursors of binary Cu/ZnO catalysts for low-pressure methanol synthesis and for the reverse water-gas shift reaction.[18−21] These procedures, in which coprecipitation takes place at very large supersaturations, usually give rise to mixed copper−zinc hydroxycarbonate phases, mainly aurichalcite and zincian−malachites;[22−26] subsequent thermal decomposition, which leads to what is believed to be a fine CuO−ZnO interdispersion, followed by reduction yields the final catalysts.[27] The importance of the nature of the precursors upon the ultimate catalyst performance has been stressed by various authors,[18,28,29] and significant work has been done to set the conditions for the synthesis of appropriate precursors.

In the present paper, we explore the possibilities of the *urea method* to prepare precursors of binary Cu/ZnO catalysts, and analyze the processes conducting to the formation of the catalysts precursors.

Experimental Section

Materials. Copper(II) nitrate (0.025 mol dm^{-3}) stock solutions were made up from $Cu(NO_3)_2 \cdot 8H_2O$, whereas those of zinc(II) nitrate (0.025 mol dm^{-3}) were prepared by dissolving the appropriate amount of $ZnCO_3$ in diluted HNO_3; the stock solutions were filtered through 0.2 μm pore size cellulose nitrate membranes and stored in plastic bottles. All reagents were analytical grade, and water was high-resistance (conductivity less than 1 μS cm^{-1}) organics-free.

In all cases, glassware was washed using a sulfonitric acid solution, rinsed with distilled water, and steam-cleaned thoroughly to avoid the presence of undesired solid particles and solutes.

Procedures. Starting solutions were prepared by mixing in a volumetric flask the necessary amounts of Cu(II) and Zn(II) stock solutions, solid urea, and water to yield the desired reactant concentrations; the pH was adjusted by small additions of NH_3. After filtration, 10 cm^3 aliquots were poured into 20 cm^3 screw-capped borosilicate test tubes, which were then placed in a thermostated water bath preheated to 363.0 ± 0.1 K. After prefixed time intervals, the tubes were withdrawn and quenched in an ice−water bath. Precipitated solids were collected by filtration through 0.2 μm pore size cellulose nitrate membranes, repeatedly washed with cold water, and dried under vacuum at room temperature. The supernatant solutions were stored for chemical analyses.

In all experiments, the initial total metal concentration, i.e., $[Cu(II)]_0 + [Zn(II)]_0$, was kept constant at 5.0×10^{-3} mol dm^{-3}, and the zinc to total metal mole ratio, $X_{Zn} = [Zn(II)]_0/([Cu(II)]_0 + [Zn(II)]_0)$, varied between 0.06 and 0.50. The concentration of urea was always 0.5 mol dm^{-3} and the initial pH 5.0 ± 0.1. For comparison, blank experiments (hereafter called *single systems*), i.e., in the absence of Cu(II) or Zn(II), were also carried out. In what follows, all mixed systems will be labeled by their respective X_{Zn} values.

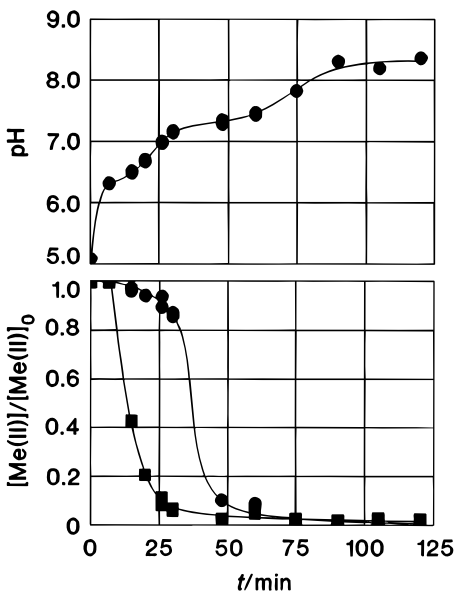

Figure 1. Time dependence of pH (upper part) and concentrations of copper (■) and zinc (●) (lower part) during the aging of the 0.50 system at 363 K; initial system composition: $[Zn(II)]_0 = [Cu(II)]_0 = 2.5 \times 10^{-3}$ mol dm^{-3}; [urea] = 0.5 mol dm^{-3}; concentrations are expressed as fractions of their initial values.

Analyses. Synthesized solids were characterized by X-ray diffraction (XRD) using Ni-filtered Cu Kα radiation ($\lambda = 1.5406$ Å), scanning electron microscopy (SEM), energy-dispersion X-ray spectroscopy (EDS), and Fourier transform infrared spectroscopy (FTIR). For EDS analysis, samples were deposited onto silver-coated glass sheets.

The concentrations of metals in the supernatant solutions were determined by atomic absorption spectrometry (AAS). All pH measurements were carried out at room temperature.

Results

Figure 1 depicts the evolution of solution composition during the aging of the 0.50 system and demonstrates that precipitation occurs in two successive steps. The first one takes place within 7−25 min aging and corresponds to copper precipitation; during this step, small amounts of zinc are gradually removed from solution (ca. less than 10%), probably by sorption onto the growing copper solid phase. The second step starts when pH raises to ca. 7.2. After 30 min aging, depletion of aqueous copper is almost complete and massive zinc precipitation, which takes about 30 min, follows.

Comparison with the precipitation behaviors of zinc and copper in their respective single systems shows that the two-step precipitation observed in Figure 1 is a consequence of the dissimilar hydrolytic properties of Cu(II) and Zn(II), the d^9 Cu^{2+} ion being more acidic than the d^{10} Zn^{2+} ion.[30] This is illustrated by Figure 2, which shows the pH dependence of dissolved Cu(II) and Zn(II) concentrations for the mixed 0.50 and the corresponding Cu- and Zn-single systems.

(18) Klier, K. *Adv. Catal.* **1982**, *31*, 243.
(19) Bulko, J. B.; Herman, R. G.; Klier, K.; Simmons, G. W. *J. Phys. Chem.* **1979**, *83*, 3118.
(20) Herman, R. G.; Klier, K.; Simmons, G. W.; Finn, P. B.; Bulko, J. B. *J. Catal.* **1979**, *56*, 407.
(21) Mehta, S.; Simmons, G. W.; Klier, K.; Herman, R. G. *J. Catal.* **1979**, *57*, 339.
(22) Himelfarb, P. B.; Simmons, G. W.; Klier, K.; Herman, R. G. *J. Catal.* **1985**, *93*, 442.
(23) Stacey, M. H.; Shannon, M. D. In *Materials Science Monographs*; Barret, P., Dufour, L.-C., Eds.; Elsevier: Amsterdam, 1985; Vol. 28B, p 713.
(24) Hoppener, R. H.; Doesburg, E. B. M.; Scholten, J. J. F. *Appl. Catal.* **1986**, *25*, 109.
(25) Pollard, A. M.; Thomas, R. G.; Williams, P. A.; Bridge, P.; Just, J. *Mineral. Mag.* **1991**, *55*, 163.
(26) Porta, P.; De Rossi, S.; Ferraris, G.; Lo Jacono, M.; Minelli, G.; Moretti, G. *J. Catal.* **1988**, *109*, 367.
(27) Porta, P.; Lo Jacono, M.; Minelli, M.; Moretti, G. *Solid State Ionics* **1989**, *32/33*, 1019.
(28) Waller, D.; Stirling, D.; Stone, F.; Spencer, M. *Faraday Discuss. Chem. Soc.* **1989**, *87*, 107.
(29) Pollard, A. M.; Spencer, M. S.; Thomas, R. G.; Williams, P. A.; Holt, J.; Jennings, J. R. *Appl. Catal. A* **1992**, *85*, 1.
(30) Baes, C. F.; Mesmer, P. E. *The Hydrolysis of Cations*; John Wiley: New York, 1976.

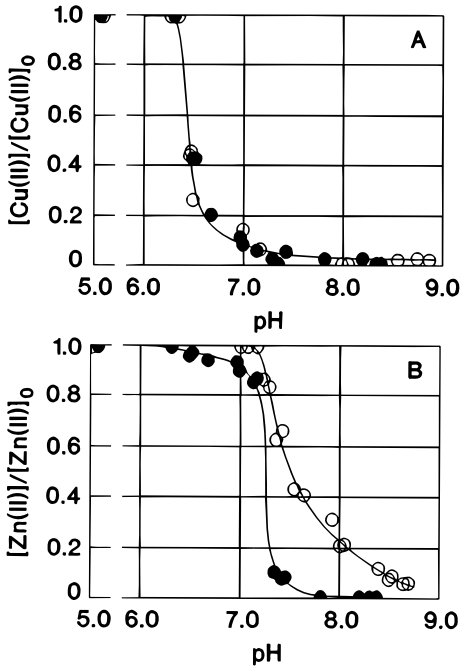

Figure 2. pH dependence of the concentrations of copper (A) and zinc (B) during the aging of the 0.50 system at 363 K; open symbols correspond to the equivalent Cu- and Zn-single systems; concentrations are expressed as fractions of their initial values.

Figure 2a indicates that zinc has no influence on the precipitation behavior of copper. Noteworthily, in the mixed 0.50 and Cu-single systems, copper removal takes place at the same pH and proceeds with the same rate. Furthermore, the precipitates collected after 30 min aging are, in both cases, amorphous copper hydroxide (*am*-$Cu(OH)_2$), the solid obtained from the 0.50 system containing small amounts of zinc.

am-$Cu(OH)_2$ was characterized by FTIR. The spectra (not shown) present a broad band, with peaks at ca. 1500 and 1400 cm^{-1} that are typical of carbonates and are assigned to the Cu−O−C stretching.[31] For various reasons, we have previously described this solid as "amorphous copper hydroxide containing variable amounts of carbonate".[12,17] Although our FTIR results are in excellent agreement with the IR spectra of georgeite (an amorphous copper basic carbonate with chemical composition similar to that of malachite),[25,29] we prefer to keep the label "*am*-$Cu(OH)_2$". Kratohvil and Matijević,[11] instead, refer to this phase as "amorphous malachite".

Although the initial precipitation stages in the mixed 0.50 and Cu-single systems are the same, the subsequent evolution of *am*-$Cu(OH)_2$ is strongly affected by the presence of Zn(II). XRD patterns show that, in the absence of Zn(II), *am*-$Cu(OH)_2$ evolves into tenorite (CuO) (Figure 3a), whereas in the 0.50 system, it transforms into aurichalcite ($Zn_{5-x}Cu_x(OH)_6(CO_3)_2$) (Figure 3b). It has been established earlier that the *am*-$Cu(OH)_2$ → CuO transformation proceeds via a dissolution−reprecipitation mechanism.[12,17] The same mechanism must operate during formation of aurichalcite; note the different crystal habits of the solids obtained after 30 and 50 min aging (Figure 4). The

(31) Nakamoto, K. *Infrared and Raman Spectra of Inorganic and Coordination Compounds*, 4th ed.; Wiley: New York, 1986; p 253.

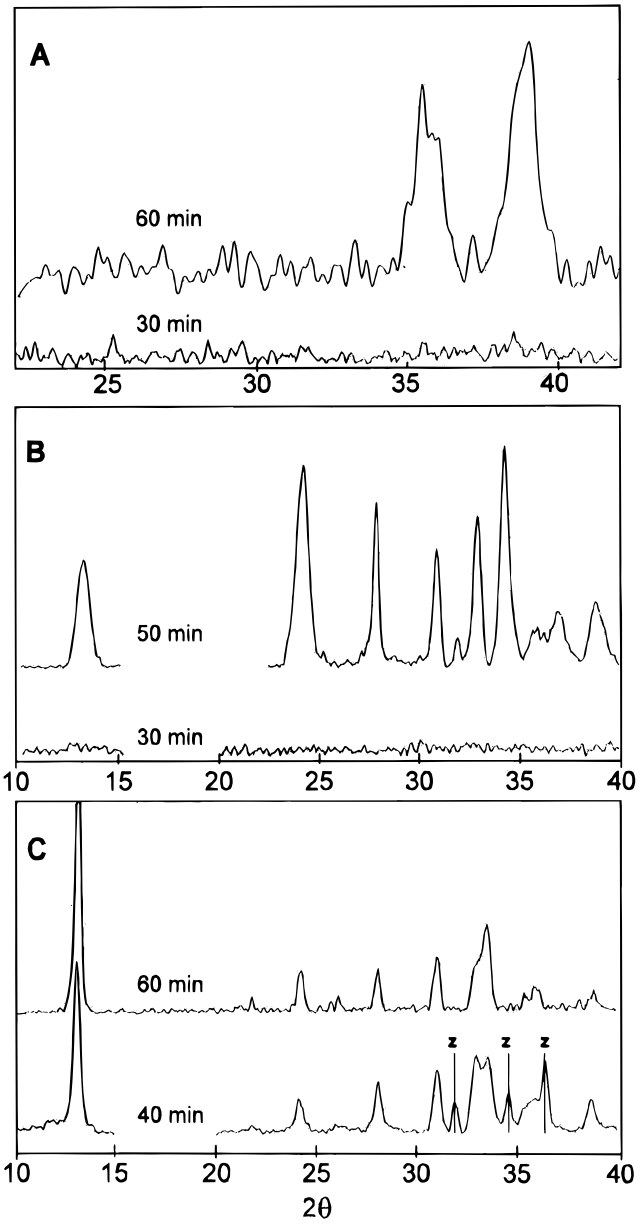

Figure 3. XRD diagrams of solids formed after short aging of the $[Cu(II)]_0 = 2.5 \times 10^{-3}$ mol dm^{-3} Cu-single system (A), the 0.50 system (B), and the $[Zn(II)]_0 = 2.5 \times 10^{-3}$ mol dm^{-3} Zn-single system (C) at 363 K; the 60 min pattern shown in A corresponds to tenorite; the 50 min pattern shown in B corresponds to aurichalcite; in C, peaks marked with a z correspond to zincite, others to hydrozincite.

actual Cu:Zn mole ratio in the final aurichalcite, determined by EDS inspection and chemical analyses, is 1.00 ± 0.05.

As compared to the Zn-single system, Cu(II) affects only slightly the early stages of aqueous zinc removal (Figure 2b); as mentioned, the influence of Cu(II) is essentially due to (ad)sorption. However, Cu(II) influences strongly the later rate of zinc precipitation. In the mixed 0.50 system, ca. 80% Zn(II) is removed from solution within 20 min after the precipitation onset (cf. Figure 1 lower), whereas in the absence of Cu(II), ca. 50 min is required to precipitate the same Zn(II) fraction. This reflects the different formation rates of aurichalcite and hydrozincite ($Zn_5(OH)_6(CO_3)_2$), the prevalent solid phase that forms in the Zn-single system (Figure 3c).

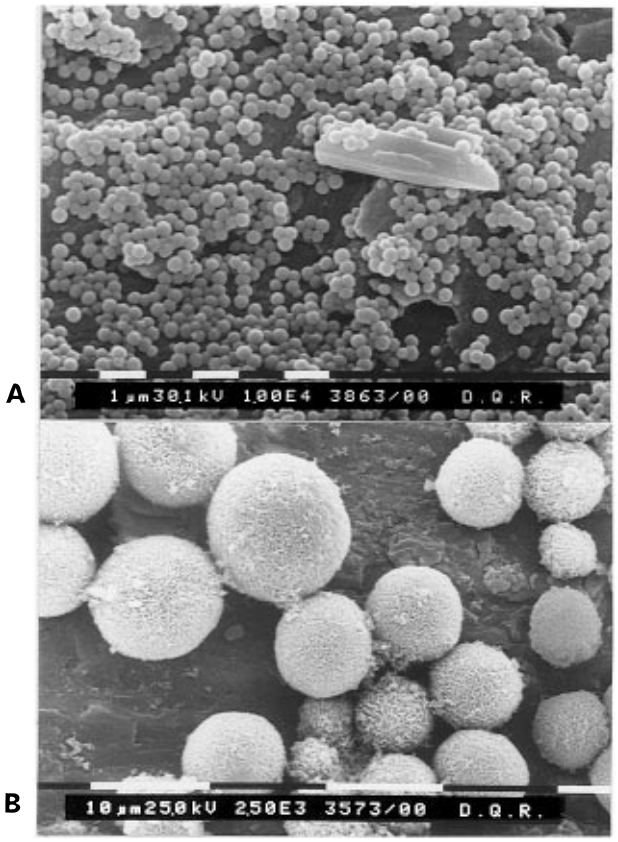

Figure 4. SEM micrographs of solids formed after the aging of the 0.50 system at 363 K for 30 (A) and 50 min (B).

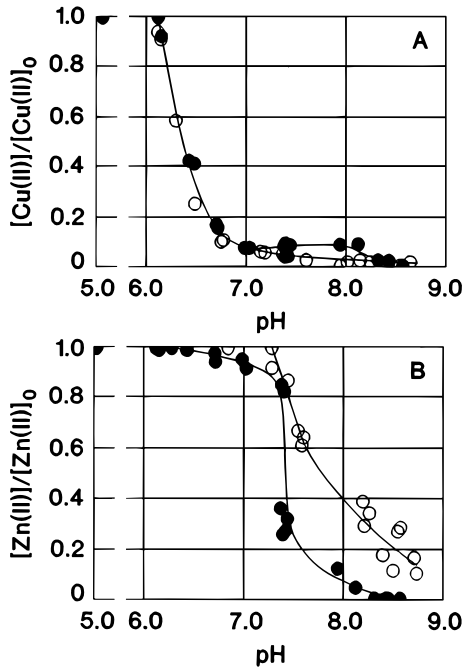

Figure 5. pH dependence of the concentrations of copper (A) and zinc (B) during the aging of the 0.30 system at 363 K; open symbols correspond to the equivalent Cu- and Zn-single systems; concentrations are expressed as fractions of their initial values.

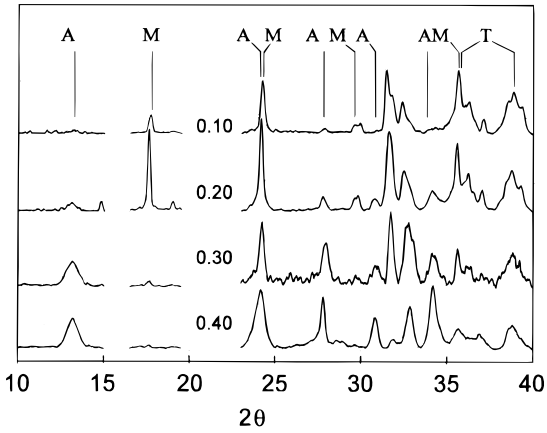

Figure 6. XRD diagrams of solids formed after 180 min aging of various mixed systems at 363 K; numbers indicate the composition of each mixed system; the letters A, M, and T indicate the position of peaks characteristic of aurichalcite, malachite, and tenorite, respectively.

The changes of solution composition during the aging of lower X_{Zn} systems resemble those presented in Figure 1. As X_{Zn} decreases, the two-step precipitation becomes even more obvious, the precipitation steps moving apart along the pH and time axes. This is a result of the increasing $[Cu(II)]_0$ to $[Zn(II)]_0$ ratio. Indeed, the pH values at which each precipitation step starts, shift with $[Cu(II)]_0$ and $[Zn(II)]_0$ in the same way they do in the equivalent single systems (cf. Figures 2 and 5). Figure 5 also illustrates the little influence of copper on the onset of massive zinc precipitation, and vice versa. Additionally, it stresses the enhancing effect of Cu(II) on the rate of aqueous zinc removal.

In all cases, the nature of the initial precipitates (i.e., those collected after 30 min aging) is the same: *am*-$Cu(OH)_2$. However, its subsequent transformation is strongly dependent on X_{Zn}. XRD information gathered in Figure 6 reveals the nature of solids synthesized after 180 min aging. Aurichalcite forms when $0.50 \geq X_{Zn} \geq 0.30$; in the latter system, however, traces of zincian−malachite ($Cu_{2-x}Zn_x(OH)_2CO_3$) become apparent. When $X_{Zn} = 0.20$, zincian−malachite prevails over aurichalcite, which is only a trace in the 0.10 system. Another important solid phase that is formed in low X_{Zn} systems (i.e., $X_{Zn} \leq 0.20$) is tenorite (actually, Zn-doped tenorite; see below). The latter findings show that the overall evolution of the precipitates formed in low X_{Zn} systems is dominated by copper; when $[Zn(II)]_0 = 0$ and $[Cu(II)]_0 > 2.5 \times 10^{-3}$ mol dm^{-3}, *am*-$Cu(OH)_2$ evolves first to $Cu_2(OH)_2CO_3$, which later transforms into CuO.[12,17] The behavior of low X_{Zn} systems is further illustrated by Figure 7, which depicts the gradual evolution of the precipitates formed in the 0.06 system. The change in the fate of the amorphous precursor, observed when $X_{Zn} \sim 0.25$ is transposed, is close to the suggested *solubility* limits of copper in aurichalcite (i.e., $Cu/(Cu + Zn) \approx 0.7$) and of zinc in zincian−malachite (i.e., $Zn/(Cu + Zn) \approx 0.2$).[23,26,28]

SEM/EDS inspection of solids formed in the 0.20 system reveals the presence of small spherical particles (ca. 0.5 μm in diameter) with $Zn/(Cu + Zn)$ ranging between 0.03 and 0.05, and of smaller irregular crystallites which form ~5 μm poorly defined aggregates with Cu:Zn mole ratios in the orders 1.5 and 4.0. Recalling the XRD data and the above-mentioned solubility limits, the nature of the observed crystallites can be easily inferred; the former particles may be identified as Zn-doped tenorite. Aurichalcite particles precipitated from the 0.40 system have a better defined shape (see Figure 8) and a Cu:Zn mole ratio which is, within the experimental error, that of the starting

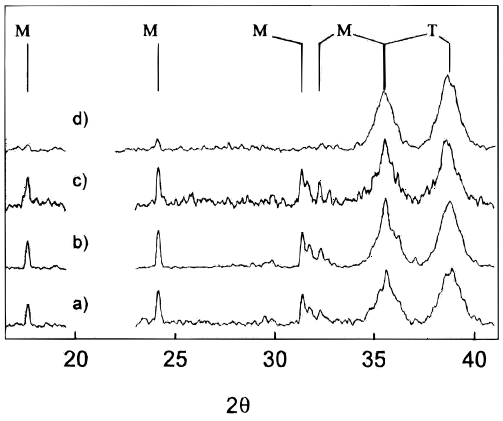

Figure 7. XRD diagrams of solids formed after aging the 0.06 system at 363 K for different periods: (a) 60, (b) 90, (c) 180, and (d) 300 min. The letters M and T indicate the position of peaks characteristic of malachite and tenorite, respectively.

solution. For the solid particles formed in the 0.06 system, the Cu:Zn mole ratio is 96:4, irrespective of their crystal structure.

Figure 8, which shows scanning electron micrographs of typical preparations, illustrates the different morphologies of the precipitates. Noteworthy, at the appropriate synthesis conditions, all basic carbonate particles form well-defined uniform spherical aggregates of small crystals. Zincian−tenorite spheres are polycrystalline, as well. Ordered aggregation and crystal growth leading to equally sized well-defined particles have been thoroughly discussed in the literature (see refs 32 and 33) and shall not be addressed here.

Discussion

As opposed to the usual coprecipitation methods used to synthesize precursors of Cu/ZnO catalysts, homogeneous alkalinization by urea hydrolysis allows for a better description of the processes leading to the formation of mixed copper−zinc hydroxycarbonates from aqueous media. The gradual increase of solution supersaturation produced by urea hydrolysis permits to differentiate the various stages through which the systems evolve. Owing to the different hard−soft nature of Cu^{2+} and Zn^{2+} ions, the observed coprecipitation behavior is somewhat complex. Thus, for the sake of clarity, we shall first present a brief analysis of the behavior of the Cu- and Zn-single systems.

Precipitation from Single Systems. The evolution of the systems can be analyzed in an approximate, albeit instructive, manner by following their trajectories along the Me(II)−H_2O−CO_2 (Me = Cu or Zn) phase diagrams; trajectories are pH vs log *C* curves (where *C* is the total carbonate concentration in the closed systems) which result from the coupling of urea hydrolysis and metal ion hydroxylation-complexation reactions that take place during aging (for details about construction of trajectories and simplifying approximations, refs 12, 15, and 17 may be consulted). The trajectories of the 2.5×10^{-3} mol dm^{-3} Cu- and Zn-single systems in the framework of their respective phase diagrams are presented in Figure 9a,b; relevant thermodynamic data have been taken from refs 30 and 34−36.

Figure 9a shows that precipitation of *am*-$Cu(OH)_2$ takes place when the solution is also supersaturated with respect to tenorite and malachite (cf. Figure 2a), a fact that reflects the Ostwald step rule (e.g., due to less stringent kinetic barriers, nucleation of less stable solid phases takes place before that of the most stable one). The trajectory then moves inside the stability domain of malachite and finally reaches that of tenorite. Consequently, *am*-$Cu(OH)_2$ evolves into CuO (Figure 3a); due to kinetic factors, malachite forms only when $[Cu(II)]_0 > 2.5 \times 10^{-3}$ mol dm^{-3}.[12,17]

Figure 9b shows that precipitation from pure zinc solutions occurs when the aqueous phase is supersaturated with respect to all considered solid phases excluding *am*-$Zn(OH)_2$ (cf. Figure 2b); at this pH value, the solution is also supersaturated with respect to ϵ-$Zn(OH)_2$. Supersaturation values, $\Omega = [Zn^{2+}]/[Zn^{2+}]_{eq}$, at the onset of precipitation are presented in Table 1. Whereas both $\Omega_{Zn_5(OH)_6(CO_3)_2}$ and Ω_{ZnCO_3} decrease with $[Zn(II)]_0$, Ω_{ZnO} and $\Omega_{\epsilon-Zn(OH)_2}$ are constant. This indicates that nucleation of ϵ-$Zn(OH)_2$ (or ZnO) is kinetically favored over that of hydrozincite or smithsonite ($ZnCO_3$). Whether ϵ-$Zn(OH)_2$ or ZnO is the actual phase that nucleates first, is an open question; the Ostwald step rule favors, however, the earlier nucleation of ϵ-$Zn(OH)_2$. Still, the overall conclusion is clear: nucleation of zinc solid phases takes place once a certain critical degree of hydroxylation has been attained.

ϵ-$Zn(OH)_2$ (or ZnO) nuclei must then act as nucleation sites for the fast heterogeneous precipitation of more stable phases, thus prompting massive precipitation. Indeed, after nucleation, the trajectory is well inside the stability domains of hydrozincite and smithsonite (Figure 9b), and ZnO rapidly disappears (Figure 3c). Formation of hydrozincite is not only thermodynamically favored (cf. Table 1) but also kinetically. The more drastic changes that are required to generate the calcite framework typical of smithsonite (where Zn^{2+} is hexacoordinated to six O atoms of CO_3^{2-})[37] from aqueous Zn(II), as compared to those required to produce the layered structure of hydrozincite (where Zn^{2+} is coordinated to both OH^- and CO_3^{2-}),[38,39] impose a larger activation barrier for $ZnCO_3$ nucleation. Furthermore, the relationship between the crystal structures of zinc hydroxide and hydrozincite[38] undoubtedly assists the heterogeneous nucleation of the latter.

It may be concluded that crystalline Zn(II) solid phases form upon precipitation more easily than those of Cu(II), a fact related again with the hydrolytic chemistry of both ions; in the case of Zn(II), the lower stability of polymeric partially hydrolyzed ions hinders the formation of an amorphous intermediate.

Precipitation from Mixed Systems. The trajectory described by the 0.50 system in the framework of the corresponding Zn(II) + Cu(II)−H_2O−CO_2 phase

(32) Ocaña, M.; Rodríguez-Clemente, R.; Serna, C. J. *Adv. Mater.* **1995**, *1*, 212.
(33) Rodríguez-Clemente, R.; Serna, C. J.; Ocaña, M.; Matijević, E. *J. Cryst. Growth* **1994**, *143*, 277.
(34) Schindler, P.; Reinert, M.; Gamsjäger, H. *Helv. Chim. Acta* **1968**, *51*, 1845.
(35) Schindler, P.; Reinert, M.; Gamsjäger, H. *Helv. Chim. Acta* **1969**, *52*, 2327.
(36) Smith, R. M.; Martell, A. E. *Critical Stability Constants*; Plenum Press: New York, 1976; Vol. 4.
(37) Wells, A. F. *Structural Inorganic Chemistry*, 3rd ed.; Clarendon Press: Oxford, 1962.
(38) Ghose, S. *Acta Crystallogr.* **1964**, *17*, 1051.
(39) Jambor, J.; Pouliot, G. *Canad. Mineral.* **1965**, *8*, 385.

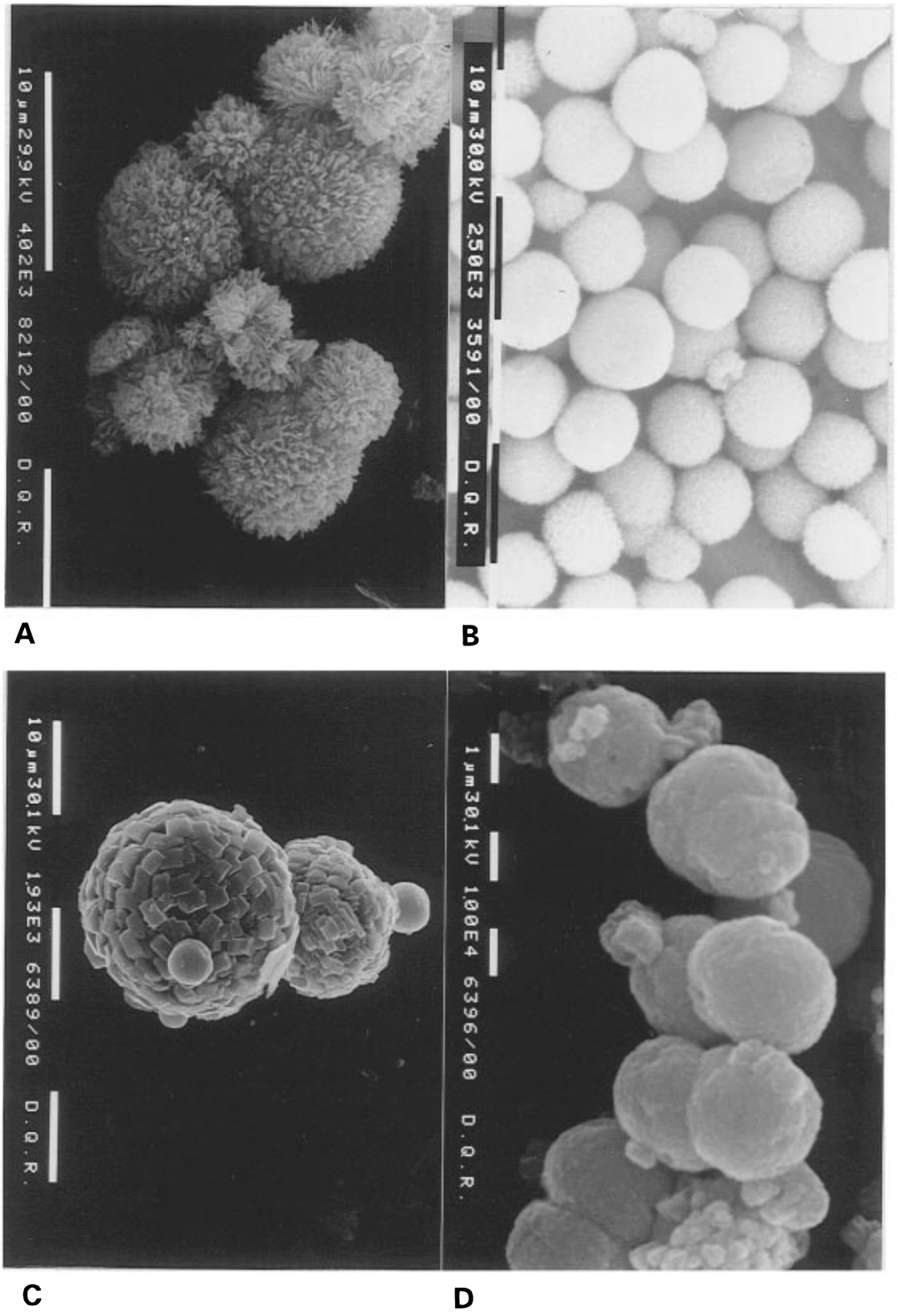

Figure 8. SEM micrographs of typical solid particles prepared by the *urea method*: (A) hydrozincite obtained after the aging of the $[Zn(II)]_0 = 2.5 \times 10^{-3}$ mol dm^{-3} Zn-single system for 180 min; (B) aurichalcite obtained after the aging of the 0.4 system for 60 min; (C) zincian−malachite obtained after the aging of the 0.06 system for 90 min (the smaller spheres are Zn-doped tenorite particles); (D) Zn-doped tenorite produced from the latter system, but aged 300 min; all systems were aged at 363 K.

diagram is shown in Figure 10; considered solid phases are $Zn_{2.5}Cu_{2.5}(OH)_6(CO_3)_2$ (for which we assume log $K_{sp} = -90.1$),[40,41] CuO, and ZnO. Comparison with Figure 9 shows that in solutions containing both $Zn(NO_3)_2$ and $Cu(NO_3)_2$ (2.5×10^{-3} mol dm^{-3}, each) aurichalcite is the most stable phase, hydrozincite and malachite being metastable. Even though the trajectory moves well inside the domain of aurichalcite from the very beginning of the aging (cf. Figure 1), this solid does not form

(40) Alwan, A. K.; Thomas, J. H.; Williams, P. A. *Trans. Met. Chem.* **1980**, *5*, 3.

(41) Smirnov, S. I. *Geochem. Int.* **1964**, *3*, 512; quoted in ref 40.

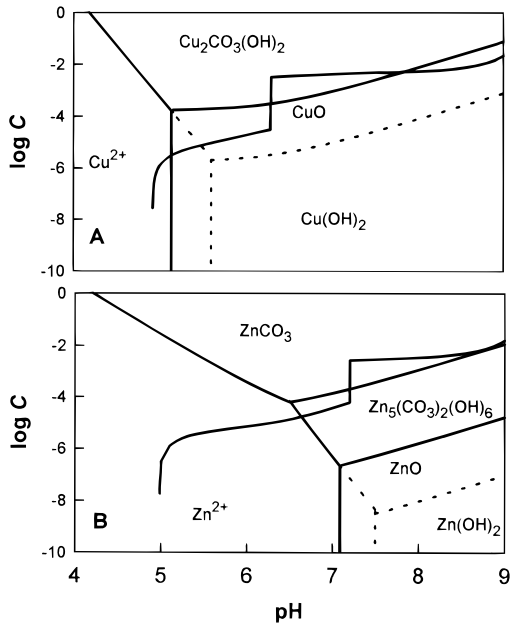

Figure 9. Trajectories described by the Cu- and Zn-single systems in the framework of their respective Me(II)−CO_2−H_2O phase diagrams; in both cases, $[Me(II)]_0 = 2.5 \times 10^{-3}$ mol dm^{-3}.

Table 1. Supersaturation Values at the Onset of Precipitation from Zinc-Single Systems[a]

$[Zn(II)]_0$ (10^3/mol dm^{-3})	2.50	1.50	1.00	0.30
pH	7.18	7.30	7.40	7.65
log (C/mol dm^{-3})	−4.22	−4.28	−4.31	−4.42
$\Omega_{\epsilon-Zn(OH)_2}$	1.1	1.1	1.2	1.1
Ω_{ZnO}	1.6	1.6	1.7	1.6
$\Omega_{Zn_5(OH)_6(CO_3)_2}$	13.7	12.2	11.6	8.0
Ω_{ZnCO_3}	6.8	4.7	3.8	1.7

[a] Onsets of precipitation were determined visually; presented pH values are interpolated values from pH vs t plots corresponding to the observed times of precipitation onset.

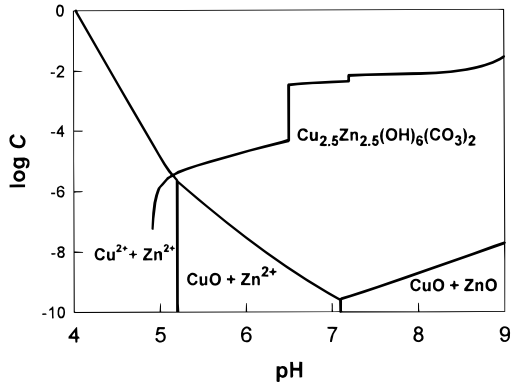

Figure 10. Trajectory described by the 0.50 system in the framework of the corresponding Cu(II) + Zn(II)−CO_2−H_2O phase diagram.

until aqueous Zn(II) attains the critical hydroxylation degree required for ϵ-$Zn(OH)_2$ nucleation (cf. Figure 2b). Again, ϵ-$Zn(OH)_2$ nuclei prompt the heterogeneous nucleation of a monoclinic zinc basic carbonate, in this case, aurichalcite; note that both hydrozincite and aurichalcite have the same crystal structure and very similar lattice parameters (a = 13.62 Å, b = 6.30 Å, c = 5.37 Å, β = 95°50′, space group $C2/m$,[38] and a = 13.82 Å, b = 6.419 Å, c = 5.29 Å, β = 101°04′, space group $P2_1/m$,[42] respectively). Interestingly, am-$Cu(OH)_2$, which precipitates first and (ad)sorbs Zn(II), does not trigger the heterogeneous nucleation of aurichalcite, a fact apparently related to the large energy requirement for dehydration of aqueous Zn^{2+}.

The growth of aurichalcite takes place at the expense of hydroxylated Zn(II) aqueous species and am-$Cu(OH)_2$ and seems to be determined by the rate of dissolution of am-$Cu(OH)_2$; due to the larger driving force, aurichalcite grows faster than hydrozincite (cf. Figure 2b). Thus, crystal growth leads to mixed copper−zinc hydroxycarbonate crystallites which later aggregate to yield the final spherical particles (Figure 4b; see also Figure 8). As a result, their in-depth composition is homogeneous, as revealed by the agreement between results from EDS and chemical analyses.

The above-mentioned kinetic factors govern also the behavior of the 0.40 and 0.30 systems (see, e.g., Figure 5), in which the rather high solubility of copper in the aurichalcite lattice[23,26,28] does not impose any other significant thermodynamic constraint. The presence of traces of zincian−malachite in the 0.30 system (Figure 6) stresses the importance of kinetics and serves to illustrate the inherent complexity that is brought about by the different hydrolytic behaviors of Cu(II) and Zn(II). As X_{Zn} is lowered, am-$Cu(OH)_2$ precipitation and aurichalcite nucleation move away. Thus, when the elapsed time is sufficient to allow for nucleation and growth of the less reactive malachite (recall the behavior of Cu-single systems), a mixture results; zincian−malachites grow by incorporation of adequately hydroxylated Zn(II) species, a process that progresses in parallel with aurichalcite precipitation.

When the solubility of copper in the aurichalcite lattice is exceeded (i.e., for systems in which X_{Zn} is lower than ca. 0.25), formation of mixtures may seem obvious (see Figure 6, XRD patterns 0.20 and 0.10), but kinetic factors are still overriding. As nicely documented by Waller et al.,[28] under the conditions of the $X_{Zn} \leq 0.20$ systems, aurichalcite is unstable with respect to zincian−malachites. Even so, once the critical hydroxylation degree required for massive zinc precipitation has been attained, metastable aurichalcite particles form in parallel with zincian−malachites and Zn-doped tenorite particles. The ease of aurichalcite formation, as compared to that of zincian−malachites, is also well illustrated by the data reported by Porta et al.[26]

Systems with $X_{Zn} \leq 0.20$ should lead to single-phase zincian−malachite powders only if malachite is stabilized with respect to tenorite (e.g., by decreasing the initial pH), for the metastable aurichalcite must dissolve upon aging; simultaneous Ostwald ripening of low zincian−malachites must also conduct to high zincian−malachites (cf. ref 26).

Up to now, formation of Zn-doped tenorite from aqueous solutions has not been reported, a fact likely to be related to the different synthesis conditions that were explored. Indeed, usual coprecipitation methods set conditions under which only zincian−malachites are stable, whereas the low carbonate concentrations attained during the hydrolysis of urea allow for tenorite formation (cf. Figure 9a). In the 0.20 and 0.10 systems, Zn-doped tenorite ($Cu_{0.96\pm0.01}Zn_{0.04\pm0.01}O$) is present as a side product (Figure 6), but when the synthesis conditions are adequately modified in such a way that

(42) Harding, M. M.; Kariuki, B. M.; Cernik, R.; Cressey, G. *Acta Crystallogr.* **1994**, *B50*, 673.

the stability of zincian−malachites is reduced (cf. ref 26), it is possible to prepare pure $Cu_{0.96}Zn_{0.04}O$ powders (Figure 7). Since in all studied cases the chemical composition of Zn-doped tenorite was the same, it may be concluded that 0.04 ± 0.01 is the limit for the solubility of Zn(II) in tenorite. Such a low value is not at all surprising in view of the appreciably different crystal chemistries of ZnO and CuO; in the wurtzite structure, oxide ions form a tetrahedral coordination polyhedron around Zn^{2+} ions, while tenorite contains nearly square-planar coordinated Cu^{2+} ions in a PtS-type structure.[37] In principle, it may be thought that the synthesized Zn-doped tenorite particles are composed of finely divided ZnO "grains" dispersed in the CuO matrix. In the absence of conclusive evidence and in view of the involved dissolution−recrystallization processes (cf. Figures 7 and 8c,d), we believe, instead, that zinc ions actually occupy defect positions in the tenorite lattice; certainly, zinc is in a concentration typical of defects.

Conclusions

This work illustrates some of the inherent complexities shared by mostly employed coprecipitation methods and indicates that copper and zinc nucleation occur as separate events; the critical hydroxylation degrees that are required for massive precipitation are little affected by the presence of the second component, which, however, strongly influences crystal growth. It further demonstrates that once the appropriate experimental conditions has been set, the *urea method* is well-suited to prepare single-phase aurichalcite and Zn-doped tenorite powders. The adequate tailoring of the preparation conditions should allow for the synthesis of single-phase zincian−malachites.

Acknowledgment. This work was supported by grants from UBA (UBACyT EX036) and Fundación Antorchas. The UBA Fellowship awarded to G.J. de A.A. S.-I. is gratefully acknowledged. A.E.R. and M.A.B. are members of CONICET. The authors are indebted to M. Villegas, M. Miyagusuku (UAQ, CNEA), and the members of Grupo de Análisis de Trazas (INQUIMAE) for their assistance in SEM, EDS, and AAS measurements. Special thanks are due to Gabbo's for providing an inspiring atmosphere.

CM9602813